DEVELOPMENT OF SHAPE MORPHING KIRIGAMI HONEYCOMBS AND ACTUATION METHODS

Robin M. Neville[1], Fabrizio Scarpa[2]

[1,2]Advanced Composites Centre for Innovation and Science (ACCIS), University of Bristol, Queen's Building, University Walk, Bristol BS8 1TR, United Kingdom

[1]Email: rn7318@bristol.ac.uk, web page: bristol.ac.uk/engineering/people/robin-neville/
[2]Email: f.scarpa@bristol.ac.uk, web page: bristol.ac.uk/engineering/people/fabrizio-l-scarpa/

Keywords: Kirigami, honeycombs, morphing

ABSTRACT

This work presents techniques to design and manufacture morphing honeycomb configurations using kirigami-inspired cutting and folding techniques. Kirigami is the ancient Japanese art of cutting and folding paper that can be used to form a 2D sheet material into a 3D cellular structure. The honeycombs developed in this work differ from traditional cellular structures because of their reduced density and variable stiffness. The stiffness is dependent on the loading direction and on the type of loading, and this directionality is ideal for 1D morphing applications. Using kirigami techniques also allows actuators and geometric features to be embedded into the honeycomb to control morphing. Work has so far focused on characterising the effect of unique new geometry features on the mechanical properties of the structure, using Finite Element Analysis. The work presented in this paper focuses on developing the honeycomb's morphing capability; we present techniques for manufacturing honeycombs with a functional shape, and analysis methods to predict the honeycomb's morphing shapes.

1 INTRODUCTION

Kirigami is the ancient Japanese art of forming a 2D sheet into a 3D cellular structure by cutting and folding paper, and can be applied to engineering sheet materials to create functional cellular structures. Engineering applications already make wide use of honeycombs; these are structures made from folded and glued sheet material, and as such can be folded using Kirigami. The first known instance of a honeycomb folded using Kirigami is a patent by H. B. Dean [1], who invented a specific cutting and folding process required to fold a honeycomb. Nojima and Saito developed the mathematics linking cutting patterns to 3D structures, so that honeycombs could be designed with a useful shape [2]–[4] (Figure 1). This work builds on these techniques to produce Kirigami cellular structures, which overcome some of the limitations of traditional honeycombs such as secondary curvature and the difficulty of forming complex shapes. Using the techniques described above, we have developed a cellular structure which has significantly more flexibility than traditional honeycombs. We denominate this architecture an "open" honeycomb because it lacks a closed cell form (we follow the naming conventions of foams, which are also called "open" or "closed" depending on their cell configuration). Figure 2 features a comparison between a traditional honeycomb and an open honeycomb specifically designed for morphing, and Figure 3 shows the manufacturing process used to manufacture the honeycombs in this work. The morphing open honeycomb has several unique features made possible by the Kirigami manufacturing process. The stiff corrugated strips are connected by folds and bridges of material which allow the structure to flex easily in one direction while maintaining stiffness in the other directions. Holes were included in the 2D cutting pattern such that these are located in controlled positions in the 3D structure. Cables are threaded through the holes in such a way that different deformed shapes can be produced by tensioning different cables. These features combine to give the open honeycomb significantly different properties and behaviour to traditional honeycombs. In past work we have characterised the effect of fold angle α and fold stiffness k on the mechanical properties of the structure.

In this work we focus on developing the morphing capability of the structure. We do this in two ways:

1. A method is presented for designing useful shape open honeycombs. This is very similar to Saito’s method [4], but is a bit more complicated because there are more variables, and more room for design.
2. A method is presented for modelling the structure as a series of rigid linkages, which can be used to predict the deformed shape of the structure in response to a cable load.

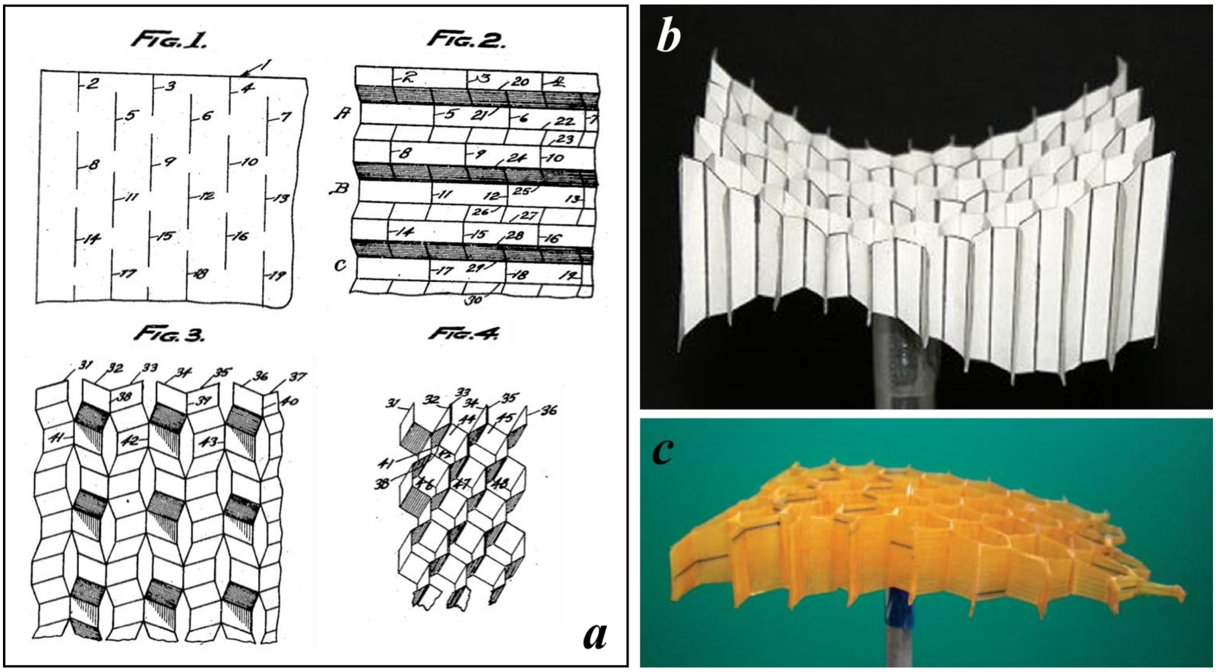

Figure 1: a) Drawings from the patent by H.B. Dean [1] showing the process of folding a honeycomb. b) & c) Functional shaped honeycombs developed by Nojima and Saito, from references [4] and [3] respectively.

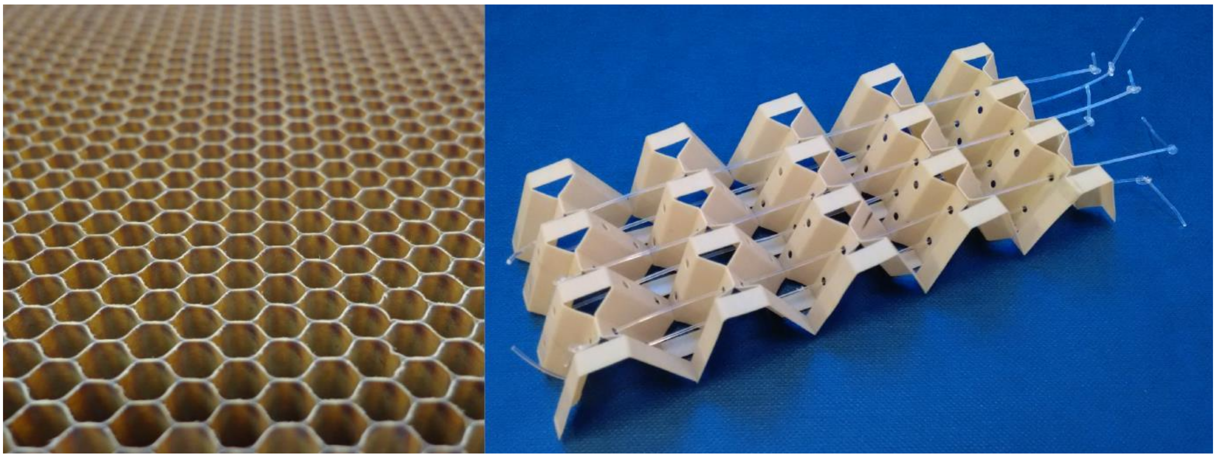

Figure 2: L: traditional honeycomb, R: open honeycomb designed for morphing with cable actuators embedded.

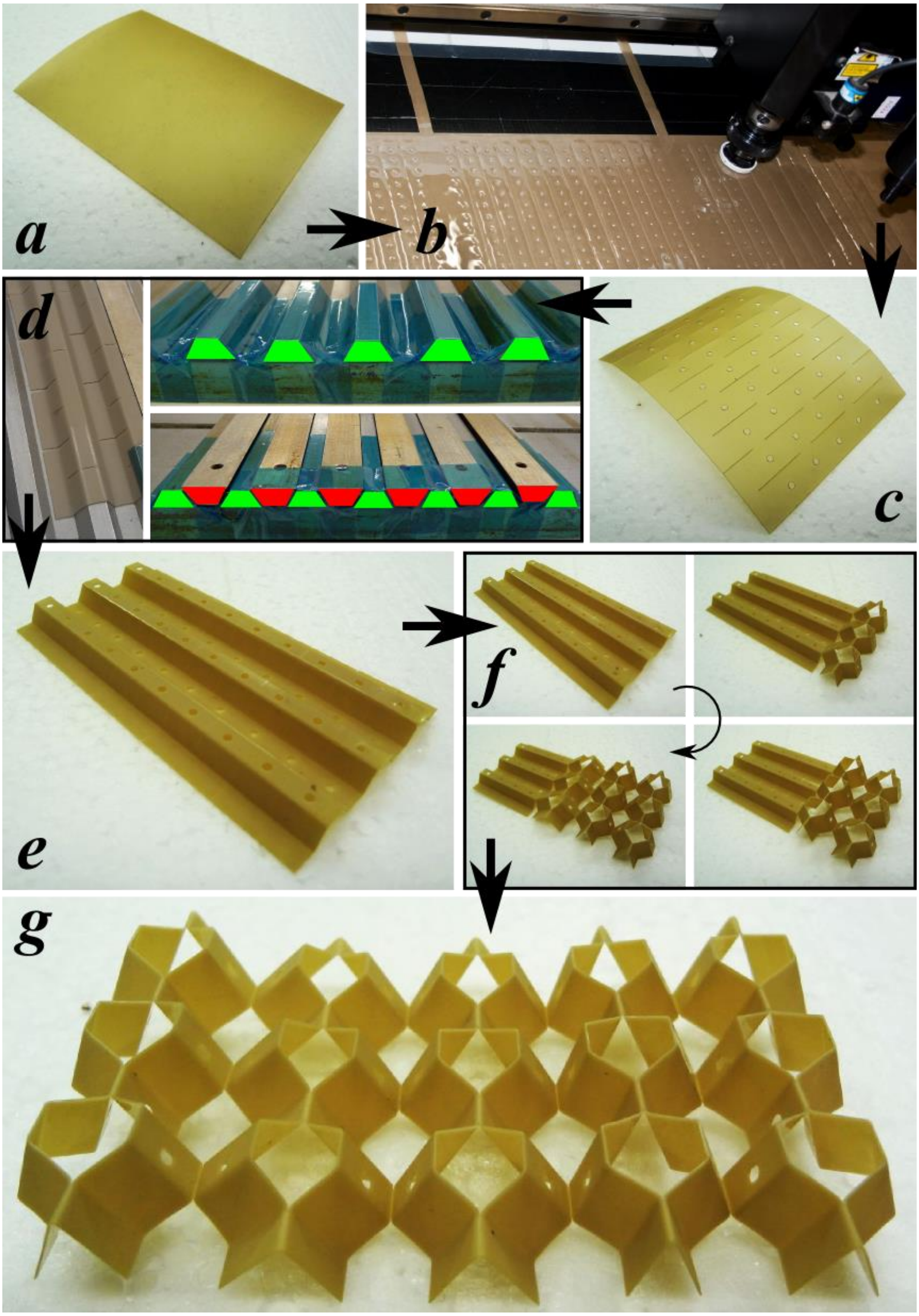

Figure 3: The Kirigami manufacturing process. a) Flat sheet. b) Cutting patterns made using a ply cutter. c) Cut sheet. d) Thermoforming between hexagonal mould rods. e) Corrugated sheet. f) Folding along the corrugations. g) Open honeycomb.

2 USEFUL SHAPE GEOMETRY

For morphing applications, we need to be able to produce a structure with a specific, useful shape e.g. an aerofoil. The 3D structure of the honeycomb is complex, but because of the orientation of the folds, it does not flex in the X direction; all of the useful morphing happens in the YZ plane. So we can analyse the structure in the YZ plane as a series of points and lines, and this makes the analysis much simpler. Figure 4 shows the dimensions of the unit cell in 2D. We now find the YZ coordinates of the points. We take point A as our starting point and give it coordinates Y_0 and Z_0, as shown in equation (1). From here we find the coordinates of points B to K using the dimensions shown in Figure 4.

$$A = [Y_A, Z_A] = [Y_0, Z_0] \tag{1}$$

$$B = [Y_B, Z_B] = A + \begin{bmatrix} +(c_1 - b_1)\sin\alpha_1 & +(c_1 - b_1)\cos\alpha_1 \\ -\dfrac{d_1\sin(\alpha_1+\beta_1)}{\sin\beta_1} \quad , & -\dfrac{d_1\cos(\alpha_1+\beta_1)}{\sin\beta_1} \end{bmatrix} \tag{2}$$

$$C = [Y_C, Z_C] = B + [b_1\sin\alpha_1 \quad , \quad b_1\cos\alpha_1] \tag{3}$$

$$D = [Y_D, Z_D] = C + \left[\frac{d_1\sin(\alpha_1+\beta_1)}{\sin\beta_1} \quad , \quad \frac{d_1\cos(\alpha_1+\beta_1)}{\sin\beta_1}\right] \tag{4}$$

$$E = [Y_E, Z_E] = C + [\chi_1\sin\phi_1 \quad , \quad \chi_1\cos\phi_1] \tag{5}$$

$$F = [Y_F, Z_F] = E + [+b_2\sin\alpha_2 \quad , \quad b_2\cos\alpha_2] \tag{6}$$

$$G = [Y_G, Z_G] = F + \left[\frac{d_2\sin(\alpha_2+\beta_2)}{\sin(\beta_2)} \quad , \quad \frac{d_2\cos(\alpha_2+\beta_2)}{\sin(\beta_2)}\right] \tag{7}$$

$$H = [Y_H, Z_H] = G + [-c_2\sin\alpha_2 \quad , \quad -c_2\cos\alpha_2] \tag{8}$$

$$I = [Y_I, Z_I] = G + [\chi_2\sin\phi_2 \quad , \quad \chi_2\cos\phi_2] \tag{9}$$

$$J = [Y_J, Z_J] = B + [e_1\sin\alpha_1 \quad , \quad e_1\cos\alpha_1] \tag{10}$$

$$K = [Y_K, Z_K] = E + [e_2\sin\alpha_2 \quad , \quad e_2\cos\alpha_2] \tag{11}$$

Having found the coordinates of all the points, we can now use these to generate equations to constrain the honeycomb to a useful shape. We choose two functions f_1 and f_2 to describe the desired lower and upper surface of the honeycomb, respectively. Figure 5 shows how 8 equations are generated for each unit cell, by constraining the points B to I to lie on f_1 or f_2. This allows us to solve for up to 8 unknowns in the system of equations. There are 14 dimensions for the whole unit cell (not counting e_1 or e_2; these are not yet used), so we must fix 6 dimensions to obtain a solution. $d_{1,2}$ are already fixed by the dimensions of the moulds used in manufacture. This leaves us with 4 dimensions to fix. The choice of constraints gives us some freedom of design. In this paper we fix $\alpha_{1,2}$ and $\chi_{1,2}$ to generate honeycombs with regular geometry. Once the YZ coordinates of the points have been found, the X coordinates are easily calculated using the dimensions of the mould rods. Figure 6 shows an example honeycomb in both 2D and 3D.

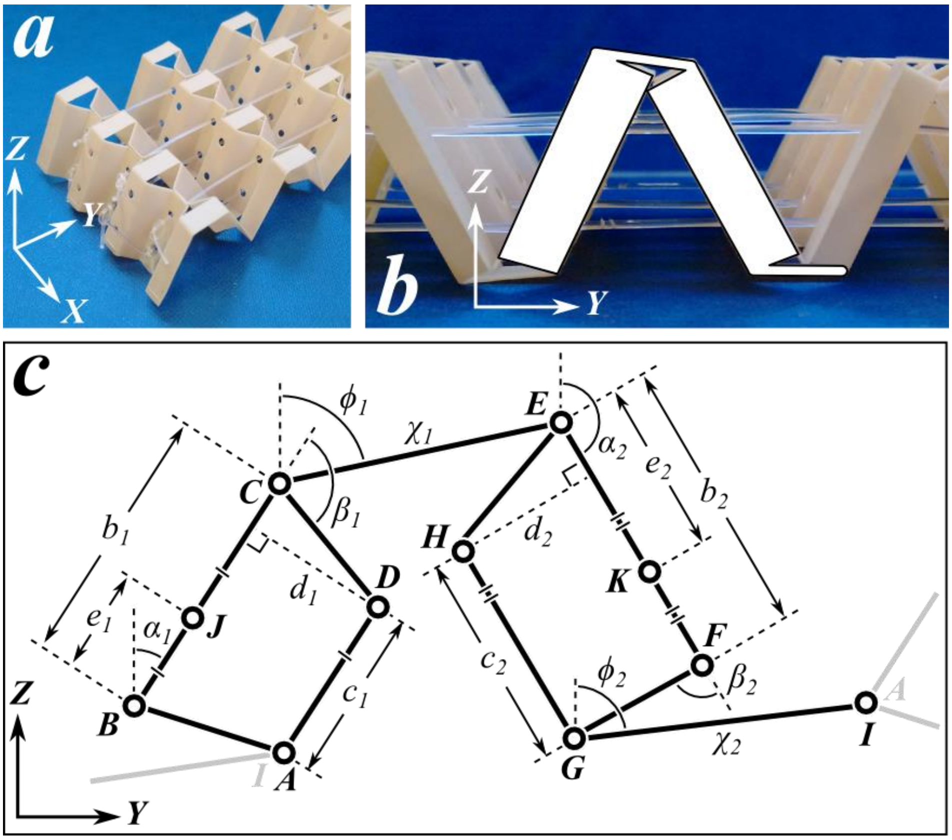

Figure 4: 2D model of the open honeycomb unit cell. a) View of the open honeycomb showing the axes directions. b) Side view of the YZ plane, with unit cell highlighted. c) Unit cell represented by points and lines in the YZ plane, showing dimensions. Parts of the adjacent cells are shown in grey. Points J and K represent locations of holes in the cell walls.

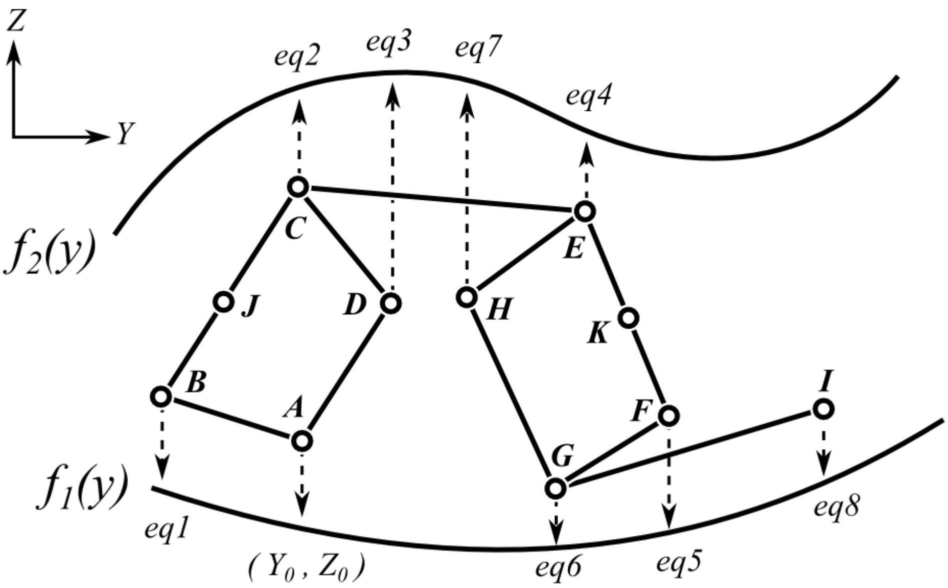

Figure 5: Equations generated by constraining points to lie on functions.

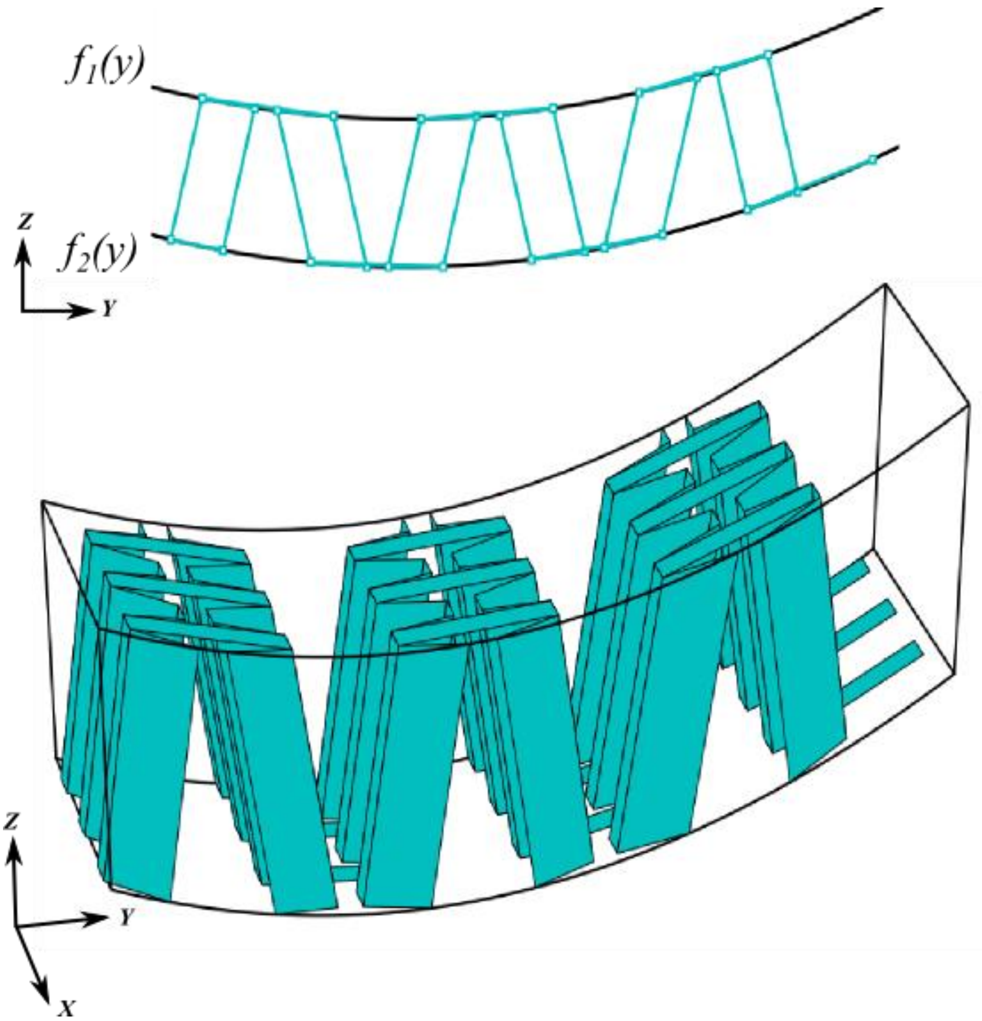

Figure 6: Honeycomb fit between two functions. Functions used were $f_1 = 0.005y^2$, $f_2 = 0.005y^2 + 10$. The four dimensions fixed manually were $\alpha_1 = 15°$, $\alpha_2 = 165°$, $\chi_1 = \chi_2 = 2.5\, l \cos\theta$ (where $l = 5mm$, $\theta = 30°$ as determined by the mould rods).

3 DEFORMED SHAPE WITH CABLE TENSION

We have shown a method to produce a honeycomb with a functional shape, and we have shown how the Kirigami process can be used to embed cable actuators into the structure. In this section we demonstrate a method to model the deformation of the structure in response to cable tension. We assume that the corrugated strips remain rigid, and that the structure deforms purely by rotating about the folds (this is a reasonable assumption because the corrugated strips are much stiffer than the folds). Given this assumption, we can idealise the corrugated strips as rigid beams, with the folds represented as rotational springs. We can then find the forces and moments at each fold, and from these we can calculate the deflections. Figure 7 shows the idealisation of the unit cell, with forces and moments. By considering each beam element starting from GI, and working backwards through the structure, we can find the forces and moments at the folds A, C, E, G in terms of the external forces and the lengths and angles of each beam. We represent these in matrix form in equation (12) (i is the cell number, and $j = A, C, E, G$).

$$\{M_j\}_i = [C_M]_i \, \{F_{ext}\}_{\mathrm{i}} \tag{12}$$

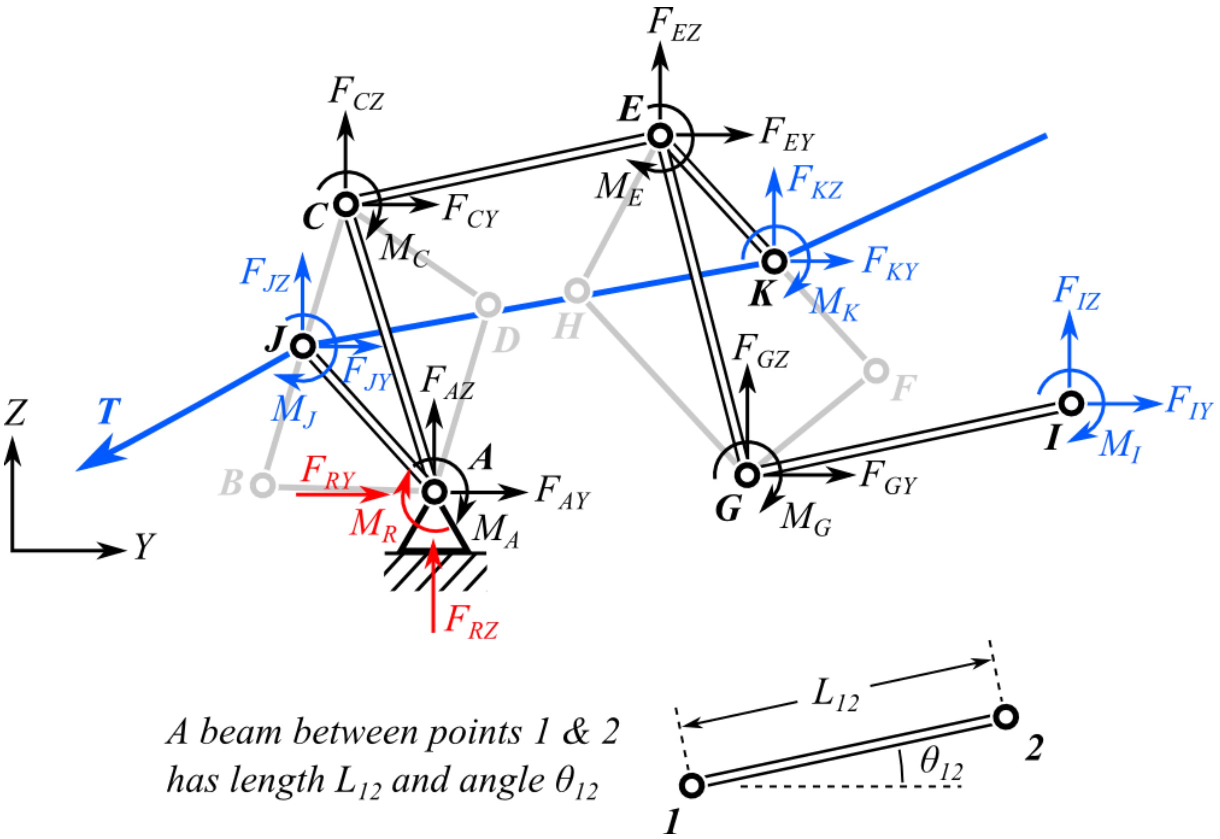

Figure 7: The unit cell idealised as a series of beams. The large blue line represents the cable with tension T. External applied forces are blue. Internal fold forces are black. External reaction forces are red. For clarity, lengths and angles of each beam are not shown. They are defined as shown in the bottom insert, with the angle measured positive counterclockwise from the Y axis.

$[C_M]$ is a matrix of coefficients made up of cell dimensions. Treating each fold as a linear rotational spring with relationship $\gamma = M/k$, the fold deflections γ_j are given by:

$$\begin{aligned} \{\gamma_j\}_i &= \{1/k_j\}_i \{M_j\}_i \\ \begin{Bmatrix} \gamma_A \\ \gamma_C \\ \gamma_E \\ \gamma_G \end{Bmatrix}_i &= \begin{Bmatrix} 1/k_A \\ 1/k_C \\ 1/k_E \\ 1/k_G \end{Bmatrix}_i \begin{Bmatrix} M_A \\ M_C \\ M_E \\ M_G \end{Bmatrix}_i \end{aligned} \tag{13}$$

We substitute (12) into (13) to obtain:

$$\{\gamma_j\}_i = \{1/k_j\}_i [C_M]_i \{F_{ext}\}_\mathrm{i} \tag{14}$$

We now have the deformation of each fold in terms of known parameters (stiffnesses $\{k_j\}$, cell geometry in $[C_M]$, and external forces $\{F_{ext}\}$). We can now find the absolute values of the fold angles measured from the vertical. We denote undeformed dimensions with a superscript “0”, and deformed dimensions with a superscript “*”. We find the deformed fold angles $\{\theta_j\}_i^* = \{\alpha_1, \phi_1, \alpha_2, \phi_2\}_i^*$ by adding the deformations $\{\gamma_j\}_i$ to the undeformed fold angles $\{\theta_j\}_i^0 = \{\alpha_1, \phi_1, \alpha_2, \phi_2\}_i^0$. The matrix $[C]$ accounts for the fact that point j experiences its deformation plus the deformations of the previous points.

$$\{\theta_j\}_i^* = \{\theta_j\}_i^0 + [C]\{\gamma_j\}_i$$
$$\begin{Bmatrix}\alpha_1\\ \phi_1\\ \alpha_2\\ \phi_2\end{Bmatrix}_i^* = \begin{Bmatrix}\alpha_1\\ \phi_1\\ \alpha_2\\ \phi_2\end{Bmatrix}_i^0 + \begin{bmatrix}1&0&0&0\\1&1&0&0\\1&1&1&0\\1&1&1&1\end{bmatrix}\begin{Bmatrix}\gamma_A\\ \gamma_C\\ \gamma_E\\ \gamma_G\end{Bmatrix}_i \tag{15}$$

This gives us the deformed fold angles in response to cable tension for one cell i. We now expand this to multiple cells. Adjacent cells i and $i+1$ are joined by point I_i meeting point A_{i+1} (see the grey lines in Figure 4). We must account for moments and deformations accumulating throughout the entire structure as well as through the cells. The fold forces and moments at point A_{i+1} act on cell i as the "external forces" at point I_i. For the final cell in the chain, N, external forces at point I_N will be zero. Deformations are summed along the structure in a similar way to how they are summed along a cell. Cell i experiences its deformations plus those of previous cells. This is represented in matrix form for N cells:

$$\begin{Bmatrix}\{\theta_j\}_1\\ \{\theta_j\}_2\\ \vdots\\ \{\theta_j\}_N\end{Bmatrix}^* = \begin{Bmatrix}\{\theta_j\}_1\\ \{\theta_j\}_2\\ \vdots\\ \{\theta_j\}_N\end{Bmatrix}^0 + \begin{Bmatrix}[C]\{\gamma_j\}_1\\ [C]\{\gamma_j\}_2\\ \vdots\\ [C]\{\gamma_j\}_N\end{Bmatrix} + \begin{bmatrix}0&0&\cdots&0\\1&0&\cdots&0\\ \vdots&\vdots&\ddots&\vdots\\1&1&\cdots&0\end{bmatrix}\begin{Bmatrix}\Sigma_j\{\gamma_j\}_1\\ \Sigma_j\{\gamma_j\}_2\\ \vdots\\ \Sigma_j\{\gamma_j\}_N\end{Bmatrix} \tag{16}$$

$$\text{Where} \begin{bmatrix}0&0&\cdots&0\\1&0&\cdots&0\\ \vdots&\vdots&\ddots&\vdots\\1&1&\cdots&0\end{bmatrix} = D$$

We now have the deformed structure fold angles in terms of fixed geometry dimensions and cable tension T. These can be substituted into equations (1)-(11) to find the deformed coordinates of points A-K. At this point we could input a value for T and find the deformed geometry, but it would be more useful to be able to specify a cable displacement δ_{cable}, since the role of a morphing structure is to assume a specific deflection. We must generate one equation so that we can specify δ_{cable} and solve for T. If we were to pull a section of cable with length δ_{cable} out of the undeformed structure to produce a deformed shape, the length of cable left inside the deformed structure would be given by:

$$L_{cable}^* = L_{cable}^0 - \delta_{cable} \tag{17}$$

Where L_{cable} is the length of cable inside the structure. We can find L_{cable} from the sum of the distances between the various points J and K throughout the cells:

$$L_{cable} = \left(\sum_i^{2:N} |K_{i-1}J_i| + |J_iK_i|\right) + |J_1K_1| \tag{18}$$

We have J^0 and K^0 because they are fixed by our choice of e_1 and e_2, and we have J^* and K^* in terms of T; thus we can specify a displacement δ_{cable} and solve (17) for T. Figure 8 shows the predicted displacement for a flat honeycomb compared to the displacement of a real honeycomb.

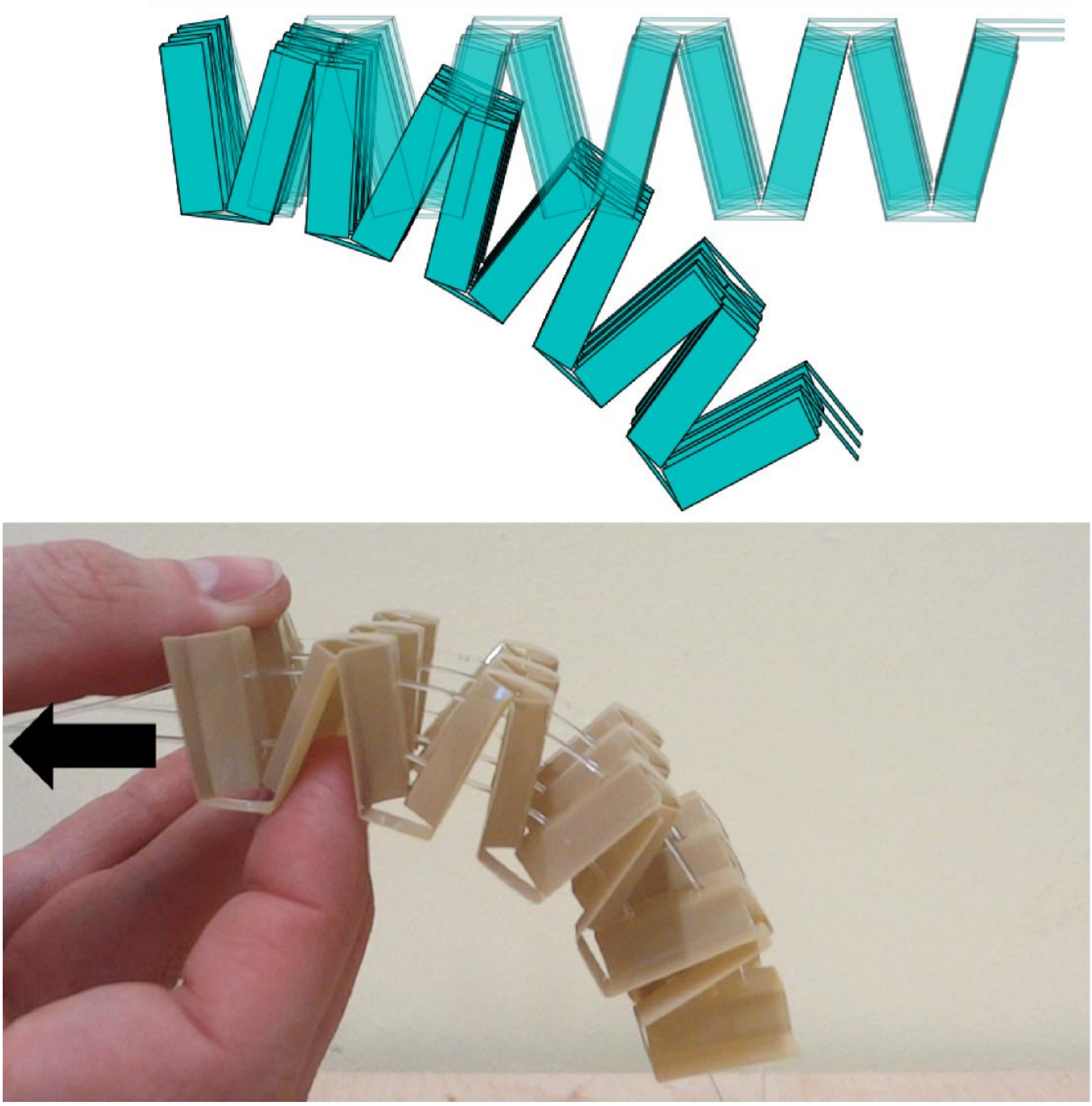

Figure 8: Comparison between predicted deflection (top) and actual deflection (bottom) when subjected to a similar cable load. The transparent plot shows the undeformed structure.

4 DISCUSSIONS

We have demonstrated several methods to a) manufacture an open honeycomb, b) design an open honeycomb with a functional shape, and c) predict the deformation of the open honeycomb in response to cable loads. We have given some basic examples to illustrate this. In this section we discuss the potential to build on these techniques by adding more functionality.

4.1 Other inserts

Future work will look at implementing other inserts besides cables. Axially stiff rods/plates and outer skin elements are all of interest. It is feasible to embed stiff rod elements into the honeycomb in much the same way as the cables. These rods could prevent the honeycomb contracting in the Y direction and encourage instead a bending motion about the X axis. Rod elements could be implemented mathematically as an equation specifying a fixed distance between two points. A compliant outer skin could be modelled by spring elements between adjacent points on the upper/lower surface.

4.2 Multiple useful shapes

If the cable inside the structure is pulled far enough, the structure will contract until the adjacent strips begin to touch one another, locking it in place. By controlling the length of the bridges between strips it may be possible to tailor this collapsed configuration to a second useful shape.

4.3 Refined structural analysis

Future work will include a more refined analysis of the full 3D structure using Finite Element Analysis. This will capture important details such as stresses at the folds and actuator load introduction points.

5 CONCLUSIONS

We have presented a method for producing open honeycombs with useful geometries, and predicting the deformation of the structure in response to embedded actuators. Future work will investigate the potential of other actuators/structural inserts, and further tailoring of the shape of the honeycomb.

ACKNOWLEDGEMENTS

Special thanks go to Mr. Ian Chorley (ACCIS Technician) for his help and advice in manufacturing the PEEK honeycombs. The Authors are also grateful to Dr. Alan Wood from Victrex plc for the advice provided about the processing of the PEEK films. The Authors would also like to thank Dr. Ian Farrow for encouraging the investigation into open honeycombs. The Authors acknowledge the Engineering and Physical Sciences Research Council for supporting this work through the Centre for Doctoral Training in Advanced Composites at the University of Bristol, UK (Grant no. EP/G036772/1).

REFERENCES

[1] H. B. Dean, “Artificial Honeycomb,” 1921.

[2] T. Nojima and K. Saito, “Development of Newly Designed Ultra-Light Core Structures,” *JSME Int. J. Ser. A*, vol. 49, no. 1, pp. 38–42, 2006.

[3] K. Saito, F. Agnese, and F. Scarpa, “A Cellular Kirigami Morphing Wingbox Concept,” *J. Intell. Mater. Syst. Struct.*, vol. 22, no. 9, pp. 935–944, Aug. 2011.

[4] K. Saito, S. Pellegrino, and T. Nojima, “Manufacture of Arbitrary Cross-Section Composite Honeycomb Cores Based on Origami Techniques,” in *Proceedings of the ASME 2013 International Design Engineering Technical Conferences and Computers and Information in Engineering Conference*, 2013.